



# Synthesis of core–shell magnetic adsorbent nanoparticle and selectivity analysis for binary system dye removal



Niyaz Mohammad Mahmoodi\*

Department of Environmental Research, Institute for Color Science and Technology, Tehran, Iran

## ARTICLE INFO

### Article history:

Received 29 June 2013

Accepted 23 September 2013

Available online 29 September 2013

### Keywords:

Core–shell magnetic adsorbent nanoparticle  
Synthesis  
Dye removal  
Binary systems  
Selectivity analysis

## ABSTRACT

Core–shell magnetic adsorbent nanoparticle (CSMAN) was synthesized and used to remove dye from binary system. The characteristics of CSMAN were investigated using FTIR and SEM. Acid Red 18 (AR18), Direct Green 6 (DG6) and Direct Red 31 (DR31) were used. The effect of adsorbent dosage, dye concentration and salt on dye removal was evaluated. Kinetic and isotherm of dye adsorption followed pseudo-second order and Langmuir isotherm, respectively. The maximum dye adsorption capacity ( $Q_0$ ) was 588, 333 and 323 mg/g for AR18, DG6 and DR31, respectively. Selectivity analysis for binary system showed that the magnetic adsorbent had no selectivity.

© 2013 The Korean Society of Industrial and Engineering Chemistry. Published by Elsevier B.V. All rights reserved.

## 1. Introduction

Several industries such as paper, plastic and textile consume in their processes large amounts of water. Textile industry releases dye into natural waterways. Dyes reduce the sunlight penetration and deplete the dissolved oxygen. In addition, some toxic, mutagenic and carcinogenic intermediates were produced by different reaction such as hydrolysis and oxidation of dye. Nowadays laws of wastewater discharge are more stringent thus industries must treat their wastewater efficiently [1–5].

Adsorption of dyes is one of the most effective and simple methods. The adsorbents are from natural materials such as chitosan and or from low-cost and economically attractive synthetic materials or even wastes [6–11].

Magnetic surface modified materials have been emerging as potential alternative to traditional adsorbents. They have high capacity to remove different organic and inorganic pollutants [11–13]. Several magnetic adsorbents have been used to remove dyes [14–17].

A literature review showed that core–shell magnetic adsorbent nanoparticle (CSMAN) was not used to remove dyes from binary system. In this paper, CSMAN was synthesized and used to remove dye from single (sin.) and binary (bin.) systems (Fig. 1). Manganese

ferrite nanoparticle was synthesized and modified by (3-amino-propyl) trimethoxy silane as a core–shell magnetic adsorbent nanoparticle. The characteristics of CSMAN were investigated using Fourier transform infrared (FTIR) and scanning electron microscope (SEM). Acid Red 18 (AR18), Direct Green 6 (DG6) and Direct Red 31 (DR31) were used as model compounds. The kinetic and isotherm of dye adsorption from single and binary systems were studied. Selectivity analysis for binary system dye removal was investigated. The effect of operational parameter (adsorbent dosage, dye concentration and salt) on dye removal was evaluated in details.

## 2. Materials and methods

### 2.1. Materials

Acid Red 18 (AR18), Direct Green 6 (DG6) and Direct Red 31 (DR31) were obtained from CIBA and used without further purification. The chemical structure of dyes was shown in Fig. 2. All other chemicals were of analytical grade and achieved from Merck.

### 2.2. Synthesize of CSMAN

Manganese ferrite nanoparticle was synthesized in our laboratory. Manganese nitrate (4.90 g) and iron nitrate (13.4 g) was dissolved in 50 mL distilled water and added to aqueous mixed solution (4.2 g NaOH in 70 mL distilled water and 3 mL

\* Tel.: +98 021 22969771; fax: +98 021 22947537.

E-mail addresses: [mahmoodi@icrc.ac.ir](mailto:mahmoodi@icrc.ac.ir), [nm\\_mahmoodi@yahoo.com](mailto:nm_mahmoodi@yahoo.com), [nm\\_mahmoodi@aut.ac.ir](mailto:nm_mahmoodi@aut.ac.ir)

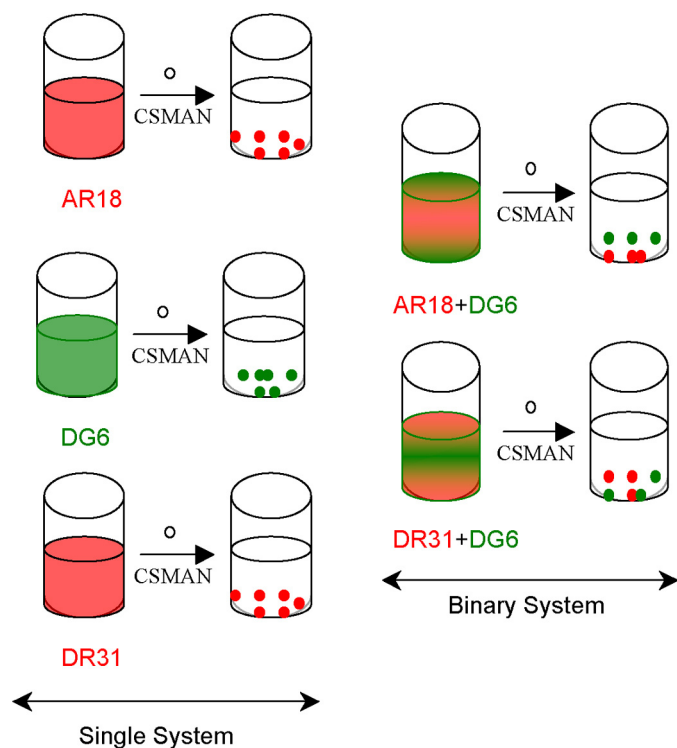


Fig. 1. Dye removal from single and binary systems using CSMAN.

ethylene diamine (EG)). This solution was heated at 90 °C for 1 h to achieve complete chelation. The powder was calcined on alumina crucible at 500 °C for 1 h, with a heating rate of 10 °C/min.

Manganese ferrite nanoparticle (1 g) and (3-aminopropyl) trimethoxy silane (2 g) were pored into mixture of water, ethanol and nonionic surfactant and mixed for 24 h at 25 °C. The precipitate was filtered, washed with deionized water and dried.

### 2.3. Characterization

The functional group of the material was studied using Fourier transform infrared (FTIR) spectroscopy (Perkin-Elmer Spectrophotometer Spectrum One) in the range 4000–450  $\text{cm}^{-1}$ . The morphological structure of the material was examined by scanning electron microscopy (SEM) using a LEO 1455VP scanning microscope.

### 2.4. Adsorption procedure

The dye adsorption measurements were conducted by mixing of CSMAN containing 250 mL of a dye solution (100 mg/L) at pH = 2.1. The change on the absorbance of all solution samples was monitored and determined at certain time intervals during the adsorption process. At the end of the adsorption experiments, the adsorbent particles were separated by magnetic force and dye concentration was determined. The results were verified with the adsorption kinetics and isotherm.

UV-vis spectrophotometer (Perkin-Elmer Lambda 25 spectrophotometer) was employed for absorbance measurements of samples. The maximum wavelength ( $\lambda_{\text{max}}$ ) used for determination of residual concentration of AR18, DG6 and DR31 in supernatant solution using UV-vis spectrophotometer were 509 nm, 634 nm and 527 nm, respectively.

The effect of adsorbent dosage on dye removal from single (sin.) and binary (bin.) systems was investigated by contacting 250 mL of

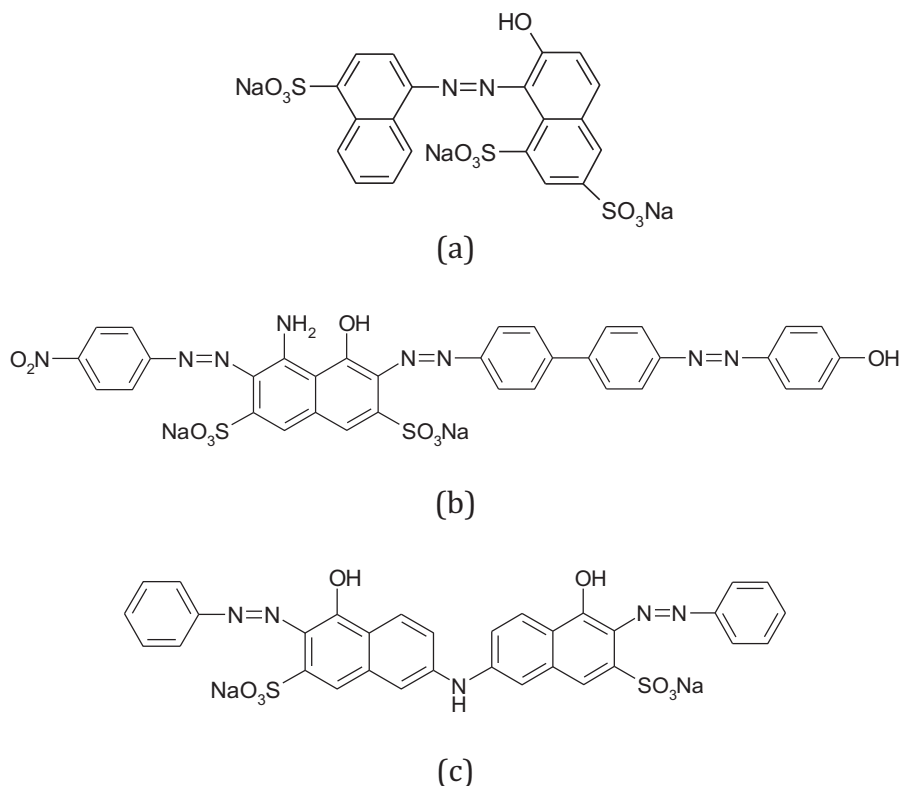


Fig. 2. The chemical structure of dyes (a) AR18, (b) DG6 and (c) DR31.

dye solution with initial dye concentration of 100 mg/L at room temperature (25 °C) for 60 min.

The effect of initial dye concentration on dye removal from single (sin.) and binary (bin.) systems was investigated by contacting 250 mL of dye solution with CSMAN at room temperature (25 °C) for 60 min.

The effect of salt (0.02 mol) on dye removal from single (sin.) and binary (bin.) systems was investigated by contacting 250 mL of dye solution (100 mg/L) with CSMAN at room temperature (25 °C) for 60 min. Different salts (NaHCO<sub>3</sub>, Na<sub>2</sub>CO<sub>3</sub> and Na<sub>2</sub>SO<sub>4</sub>) were used.

Dye concentrations in a binary system of components A and B at wavelengths of  $\lambda_1$  and  $\lambda_2$ , respectively, to give optical densities of  $d_1$  and  $d_2$  were measured as follows [18]:

$$d_1 = k_{A1}C_A + k_{B1}C_B \quad (1)$$

$$d_2 = k_{A2}C_A + k_{B2}C_B \quad (2)$$

$$C_A = \frac{k_{B2}d_1 - k_{B1}d_2}{k_{A1}k_{B2} - k_{A2}k_{B1}} \quad (3)$$

$$C_B = \frac{k_{A1}d_2 - k_{A2}d_1}{k_{A1}k_{B2} - k_{A2}k_{B1}} \quad (4)$$

where  $k_{A1}$ ,  $k_{B1}$ ,  $k_{A2}$  and  $k_{B2}$  are the calibration constants for components A and B at the two wavelengths  $\lambda_1$  and  $\lambda_2$ , respectively.

### 3. Results and discussion

#### 3.1. Adsorption kinetics

In order to study the mechanism of pollutant adsorption onto an adsorbent, characteristic constants of adsorption were determined using pseudo-first order equation [19], pseudo-second order equation [20] and intraparticle diffusion [21–23].

A linear form of pseudo-first order model is:

$$\log(q_e - q_t) = \log(q_e) - \left(\frac{k_1}{2.303}\right)t \quad (5)$$

where  $q_e$ ,  $q_t$  and  $k_1$  are the adsorbed dye at equilibrium (mg/g), the amount of the adsorbed dye at time  $t$  (mg/g) and the equilibrium rate constant of pseudo-first order kinetics (1/min), respectively.

Linear form of pseudo-second order model was illustrated as:

$$\frac{t}{q_t} = \frac{1}{k_2 q_e^2} + \left(\frac{1}{q_e}\right)t \quad (6)$$

where  $k_2$  is the equilibrium rate constant of pseudo-second order (g/mg min).

The possibility of intraparticle diffusion resistance affecting adsorption was explored by using the intraparticle diffusion model as

$$q_t = k_p t^{1/2} + I \quad (7)$$

where  $k_p$  and  $I$  are the intraparticle diffusion rate constant and intercept, respectively.

The plot of uptake should be linear when intraparticle diffusion is involved in the adsorption process. In addition, intraparticle diffusion is the rate controlling step when the lines of uptake pass through the origin then. When the plots do not pass through the origin, this is indicative of some degree of boundary layer control and it shows that the intraparticle diffusion is not the only rate limiting step, but also other kinetic models may control the rate of adsorption, all of which may be operating simultaneously [21–23].

To understand the applicability of the pseudo-first order, pseudo-second order and intraparticle diffusion models for the dye adsorption onto CSMAN from single (sin.) and binary (bin.) systems at different adsorbent dosage, linear plots of  $\log(q_e - q_t)$  versus contact time ( $t$ ),  $t/q_t$  versus contact time ( $t$ ) and  $q_t$  against  $t^{1/2}$  are plotted. The values of  $k_1$ ,  $k_2$ ,  $k_p$ ,  $I$ ,  $R^2$  (correlation coefficient values) and the calculated  $q_e((q_e)_{cal.})$  are shown in Table 1.

The linearity of the plots ( $R^2$ ) demonstrates that pseudo-first order and intraparticle diffusion kinetic models do not play a significant role in the uptake of the dye (Table 1). The linear fit between the  $t/q_t$  versus contact time ( $t$ ) and calculated  $R^2$  for pseudo-second order kinetics model show that the dye removal kinetic can be approximated as pseudo-second order kinetics (Table 1). In addition, the experimental  $q_e((q_e)_{exp.})$  values agree with the calculated ones ( $(q_e)_{cal.}$ ), obtained from the linear plots of pseudo-second order kinetics (Table 1).

#### 3.2. Adsorption isotherm

The adsorption isotherm studies the relation between the mass of the dye adsorbed onto adsorbent and liquid phase of the dye concentration [24–26].

Several isotherms such as Langmuir, Freundlich and Tempkin models were studied in details. In Langmuir isotherm, a basic assumption is that sorption takes place at specific sites within the adsorbent [27–30]. The Langmuir equation can be written as follows:

$$\frac{C_e}{q_e} = \frac{1}{K_L Q_0} + \frac{C_e}{Q_0} \quad (8)$$

where  $C_e$ ,  $K_L$  and  $Q_0$  are the equilibrium concentration of dye solution (mg/L), the Langmuir constant (L/g) and the maximum adsorption capacity (mg/g), respectively.

Isotherm data were tested with Freundlich isotherm that can be expressed by [27,31]:

$$\log q_e = \log K_F + \left(\frac{1}{n}\right) \log C_e \quad (9)$$

where  $K_F$  is adsorption capacity at unit concentration and  $1/n$  is adsorption intensity.

The Tempkin isotherm is given as:

$$q_e = B_1 \ln K_T + B_1 \ln C_e \quad (10)$$

where

$$B_1 = \frac{RT}{b} \quad (11)$$

Tempkin isotherm assumes that the heat of adsorption of all the molecules in the layer decreases linearly with coverage due to adsorbent–adsorbate interactions. Also, the adsorption is characterized by a uniform distribution of binding energies, up to some maximum binding energy [32,33]. A plot of  $q_e$  versus  $\ln C_e$  enables the determination of the isotherm constants  $B_1$  and  $K_T$  from the slope and the intercept, respectively.  $K_T$  is the equilibrium binding constant (L/mg) corresponding to the maximum binding energy and constant  $B_1$  is related to the heat of adsorption. The  $R$  and  $T$  are the gas constant (8.314 J/mol K) and the absolute temperature (K), respectively.

To study the applicability of the Langmuir, Freundlich and Tempkin isotherms for the dye adsorption onto CSMAN from single (sin.) and binary (bin.) systems at different adsorbent dosage, linear plots of  $C_e/q_e$  against  $C_e$ ,  $\log q_e$  versus  $\log C_e$  and  $q_e$  versus  $\ln C_e$  are plotted. The values of  $Q_0$ ,  $K_L$ ,  $K_F$ ,  $1/n$ ,  $K_T$ ,  $B_1$  and  $R^2$  are shown in Table 2.

**Table 1**  
Linearized kinetics coefficients of dye removal using CSMAN at different adsorbent dosages from single and binary systems.

Dye	Adsorbent (g)	$(q_e)_{Exp}$	Pseudo-first order			Pseudo-second order			Intraparticle diffusion		
			$(q_e)_{Cal.}$	$k_1$	$R^2$	$(q_e)_{Cal.}$	$k_2$	$R^2$	$k_p$	$I$	$R^2$
<b>Single system</b>											
DG6	0.025	314	105	0.038	0.981	312	0.001	0.995	15	196	0.986
	0.050	272	74	0.039	0.981	270	0.002	0.997	11	189	0.985
	0.075	245	56	0.035	0.983	244	0.003	0.998	8	1808	0.986
	0.100	225	5	0.048	0.966	226	0.004	0.999	8	166	0.922
AR18	0.025	469	349	0.052	0.980	469	0.003	0.995	49	108	0.989
	0.050	324	220	0.050	0.978	326	0.006	0.994	31	93	0.982
	0.075	272	164	0.059	0.984	270	0.009	0.992	23	109	0.974
	0.100	226	108	0.056	0.978	226	0.002	0.994	14	119	0.980
DR31	0.025	300	86	0.023	0.978	303	0.002	0.998	11	221	0.982
	0.050	251	62	0.045	0.984	250	0.003	0.998	9	183	0.983
	0.075	239	64	0.048	0.985	238	0.004	0.998	9	171	0.982
	0.100	224	67	0.060	0.987	225	0.005	0.998	9	156	0.963
<b>Binary system</b>											
<i>DG6+AR18</i>											
DG6	0.025	176	53	0.043	0.985	175	0.003	0.997	8	119	0.984
	0.050	158	52	0.047	0.987	156	0.003	0.997	7	103	0.983
	0.075	129	42	0.057	0.973	128	0.005	0.998	5	88	0.989
	0.100	117	33	0.061	0.984	116	0.006	0.999	4	85	0.973
AR18	0.025	183	45	0.044	0.987	182	0.004	0.998	6	134	0.983
	0.050	158	43	0.045	0.982	159	0.005	0.999	5	118	0.969
	0.075	129	36	0.046	0.984	129	0.004	0.997	5	83	0.982
	0.100	113	34	0.047	0.988	114	0.005	0.998	5	77	0.984
<i>DG6+DR31</i>											
DG6	0.025	179	82	0.059	0.968	179	0.002	0.995	11	101	0.983
	0.050	161	61	0.051	0.978	161	0.003	0.995	8	97	0.985
	0.075	131	38	0.047	0.987	133	0.005	0.998	5	92	0.988
	DR31	0.100	118	28	0.043	0.982	118	0.006	0.999	4	88
0.025		176	46	0.046	0.981	175	0.004	0.998	7	124	0.979
0.050		153	41	0.057	0.982	154	0.005	0.999	6	112	0.983
0.075		132	36	0.060	0.965	132	0.006	0.999	5	98	0.980
0.100	115	24	0.063	0.987	115	0.008	0.999	4	89	0.963	

The  $R^2$  values show that the dye removal isotherm using CSMAN for DG6, AR18, and DR31 in single system follows the Langmuir, Freundlich and Langmuir isotherms, respectively (Table 2). Dye removal in binary system follows the Langmuir isotherm.

The maximum adsorption capacity of several magnetic adsorbents was shown in Table 3. The results show that magnetic

nanoparticle has higher dye adsorption capability. Thus magnetic nanoparticle can be used as an adsorbent.

### 3.3. Selectivity analysis for binary system

In this research, selectivity analysis has been also performed for binary system. Usually, the static distribution coefficient  $K_D$  (mL/g)

**Table 2**  
Linearized isotherm coefficients of dye removal using CSMAN at different adsorbent dosages from single and binary systems.

System	Langmuir			Freundlich			Tempkin		
	$Q_0$	$K_L$	$R^2$	$K_F$	$1/n$	$R^2$	$K_T$	$B_1$	$R^2$
<b>Single system</b>									
DG6	333	0.120	0.981	150	0.163	0.878	3	43	0.847
	AR18								
	588								
	DR31								
323	0.110	0.978	131	0.183	0.829	34	22	0.716	
<b>Binary system</b>									
<i>DG6+AR18</i>									
DG6	192	0.280	0.984	93	0.174	0.878	29	25	0.857
	AR18								
	213								
<i>DG6+DR31</i>									
DG6	192	0.315	0.988	96	0.171	0.903	25	26	0.874
	DR31								
	200								
	0.253	0.991	86	0.197	0.973	14	28	0.951	

**Table 3**  
The dye removal ability of different magnetic adsorbents.

Magnetic adsorbent	Dye	Q <sub>0</sub> (mg/g)	Isotherm	Ref.
Magnetic alginate bead	Methylene blue	9	Freundlich	[14]
	Methyl orange	8		
Magnetic multi-wall carbon nanotube nanocomposite	Methylene blue	16	Freundlich	[15]
	Neutral red	20		
	Brilliant cresyl blue	24		
γ-Fe <sub>2</sub> O <sub>3</sub>	Acridine orange	59	Freundlich	[16]
	Multi-walled carbon nanotube filled with Fe <sub>2</sub> O <sub>3</sub>	Methylene blue	42	Freundlich
CSMAN	Neutral red	77	Langmuir	This study
	Acid Red 18	588		
	Direct Green 6	333		
	Direct Red 31	323	Langmuir	

and the separation factor  $\alpha$  are utilized to evaluate the molecular selectivity of adsorbent. Parameters  $K_D$  and  $\alpha$  are defined as follows [34]:

$$K_D = \frac{Q_e}{C_e} \quad (12)$$

The selectivity of dye in mixture is quantified by the ratio of the two partition coefficients  $K_{D1}$  and  $K_{D2}$  (for dyes 1 and 2, respectively):

$$\alpha = \frac{K_{D2}}{K_{D1}} \quad (13)$$

The higher value of  $\alpha$ , the better selectivity is; if  $\alpha$  is close to 1.0, the adsorbent has no selectivity [34].

Table 4 shows the experimental results from the adsorption experiments in binary systems. The results show that  $\alpha$  value is close to 1.0. Thus CSMAN has no selectivity.

### 3.4. Effect of operational parameter on dye removal

#### 3.4.1. Effect of adsorbent dosage

The dye removal (%) from single (sin.) and binary (bin.) systems versus time (min) at different CSMAN dosages (g) was shown in Fig. 3. The increasing of dye removal with adsorbent dosage can be attributed to increased adsorbent surface and availability of more adsorption sites. However, the capacity decreased with the increasing amount of adsorbent when the adsorption capacity was expressed in mg adsorbed per gram of material. It can be attributed to overlapping or aggregation of adsorption sites resulting in a decrease in total adsorbent surface area available to the dye and an increase in diffusion path length [35].

**Table 4**  
Selectivity analysis for binary system dye removal using CSMAN.

Binary system	Adsorbent (g/L)	Dye	$K_D$	$\alpha$
DG6 + AR18	0.025	DG6	5.444	0.946
		AR18	5.755	1.057
	0.050	DG6	8.543	0.990
		AR18	8.628	1.010
	0.075	DG6	11.293	0.999
		AR18	11.300	1.001
0.100	DG6	38.084	1.612	
	AR18	23.623	0.620	
DG6 + DR31	0.025	DG6	5.557	1.025
		DR31	5.419	0.975
	0.050	DG6	9.033	1.145
		DR31	7.890	0.873
	0.075	DG6	12.457	0.983
		DR31	12.669	1.017
0.100	DG6	42.790	1.440	
	DR31	29.716	0.694	

#### 3.4.2. Effect of dye concentration

The dye removal (%) from single (sin.) and binary (bin.) systems versus time (min) at different dye concentrations (mg/L) was shown in Fig. 4. The dye adsorption onto adsorbent increases with an increase in the initial dye concentration of solution if the amount of adsorbent is kept unchanged due to the increase in the driving force of the concentration gradient with the higher initial dye concentration. The adsorption of dye by adsorbent is very intense and reaches equilibrium very quickly at low initial concentrations. At a fixed adsorbent dosage, the amount of dye adsorbed increased with increasing concentration of solution, but the percentage of adsorption decreased. In other words, the residual dye concentration will be higher for higher initial dye concentrations. In the case of lower concentrations, the ratio of initial number of dye moles to the available adsorption sites is low and subsequently the fractional adsorption becomes independent of initial concentration [36–40].

#### 3.4.3. Effect of salt

The salts exist in water and wastewater [2]. Inorganic anions of salts may compete for the active sites on the adsorbent surface or deactivate the adsorbent. Thus dye adsorption efficiency decreases. An important limitation resulting from the high reactivity and non-selectivity of adsorbent is that it also reacts with non-target compounds present in the wastewater such as dye auxiliaries present in the exhausted reactive dye bath. It results higher adsorbent dosage demand to accomplish the desired degree of dye removal efficiency.

To investigate inorganic salts effect on dye removal efficiency, NaHCO<sub>3</sub>, Na<sub>2</sub>CO<sub>3</sub> and Na<sub>2</sub>SO<sub>4</sub> were used. Fig. 5 illustrates that dye removal capacity of CSMAN from single (sin.) and binary (bin.) systems decreases in the presence of inorganic anions because small anions compete with dyes in adsorption by magnetic nanoparticle.

### 3.5. Characterization of CSMAN

In order to investigate the surface characteristics of magnetic nanoparticle, FTIR in the range 4000–450 cm<sup>-1</sup> and SEM were studied. The FT-IR spectrum of manganese ferrite nanoparticle and CSMAN was shown in Fig. 6. Manganese ferrite nanoparticle has two peaks at 3450 cm<sup>-1</sup> and 600–500 cm<sup>-1</sup> which indicate O–H stretching vibration and metal–oxygen vibration, respectively (Fig. 6a). The FTIR spectrum of CSMAN (Fig. 6b) shows bands at 3435 cm<sup>-1</sup>, and 2927 cm<sup>-1</sup>, 2864 cm<sup>-1</sup>, 1560 cm<sup>-1</sup>, and 1120 cm<sup>-1</sup>. These bands are assigned to N–H stretching vibration, –CH<sub>2</sub>– asymmetric vibration, –CH<sub>2</sub>– symmetric vibration, C–N (amine) bending vibration, and C–N stretch (aliphatic amine), respectively [41]. The band at and 1025 cm<sup>-1</sup> is attributed to stretching vibration of Si–O–Metal [42].

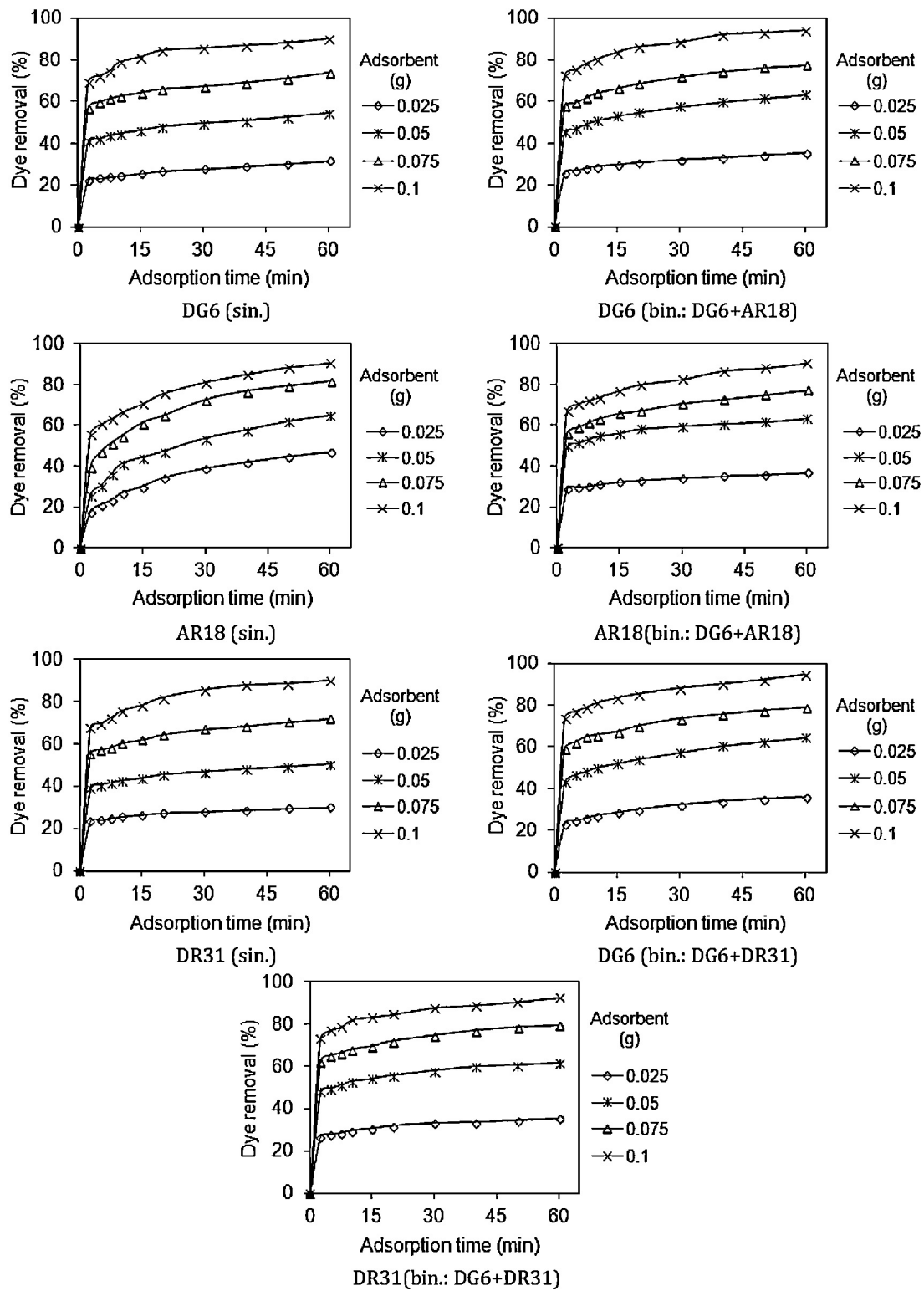


Fig. 3. The effect of adsorbent dosage on dye removal by CSMAN from single (sin.) and binary (bin.) systems.

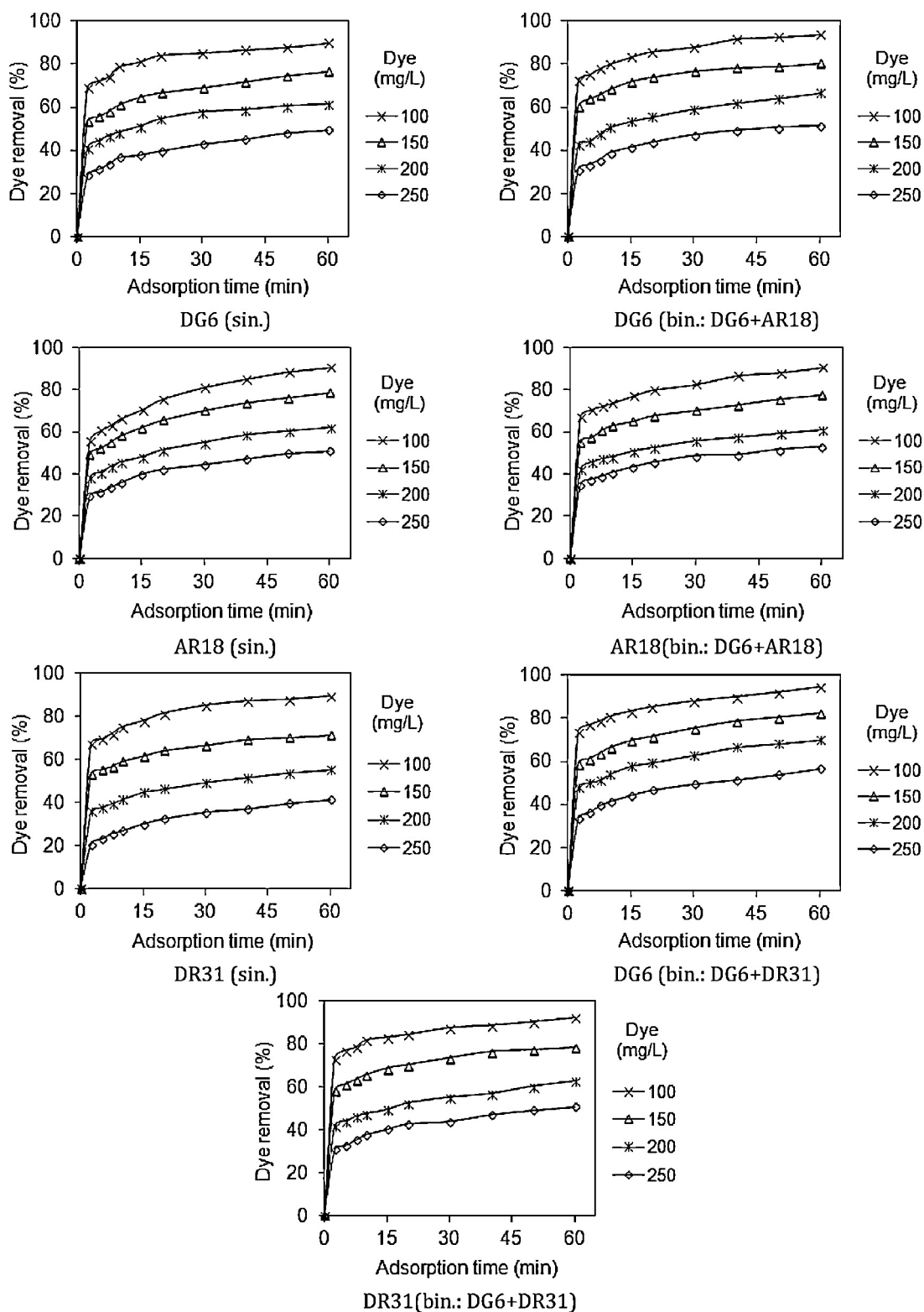


Fig. 4. The effect of dye concentration on dye removal by CSMAN from single (sin.) and binary (bin.) systems.

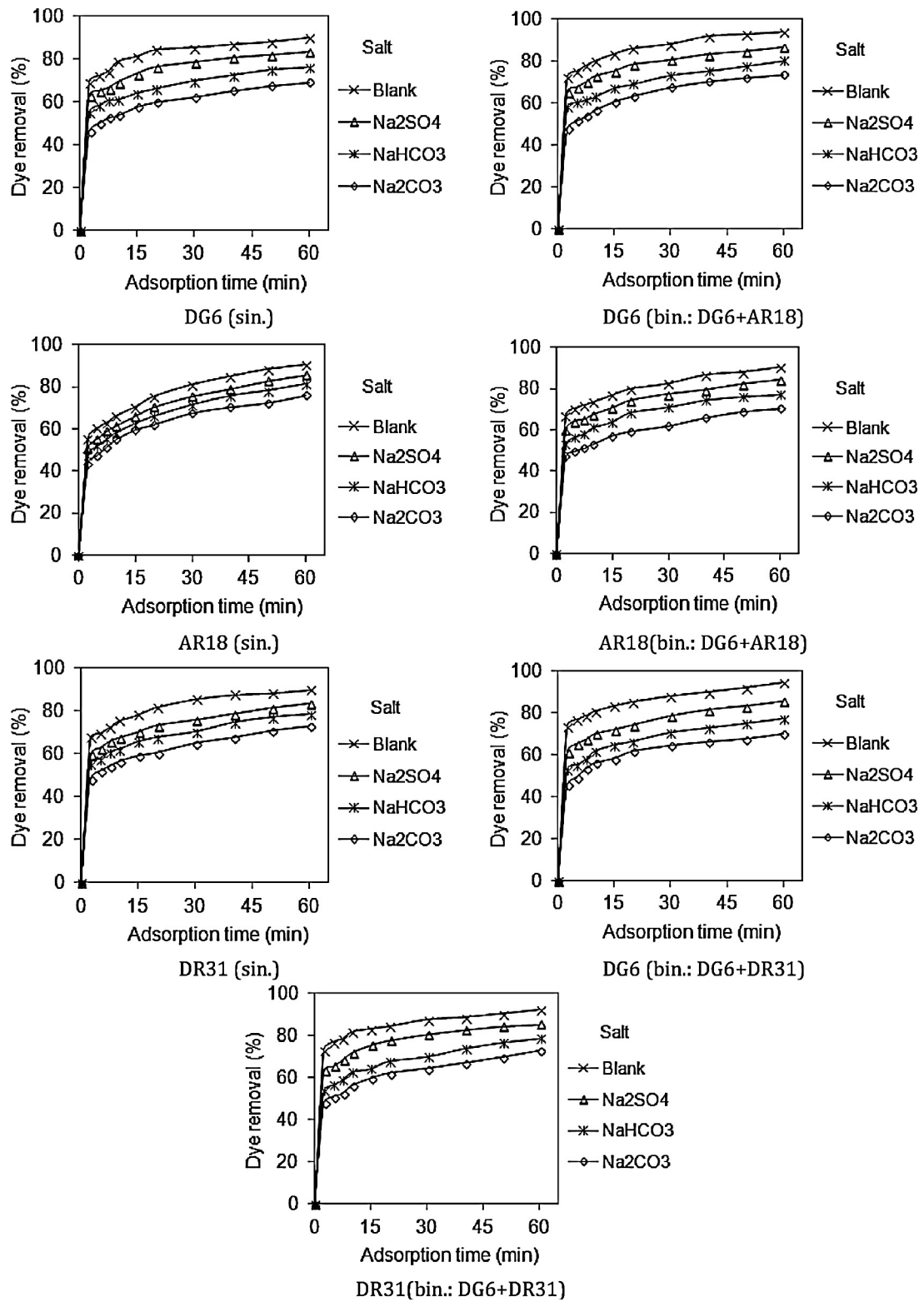


Fig. 5. The effect of salt on dye removal by CSMan from single (sin.) and binary (bin.) systems.

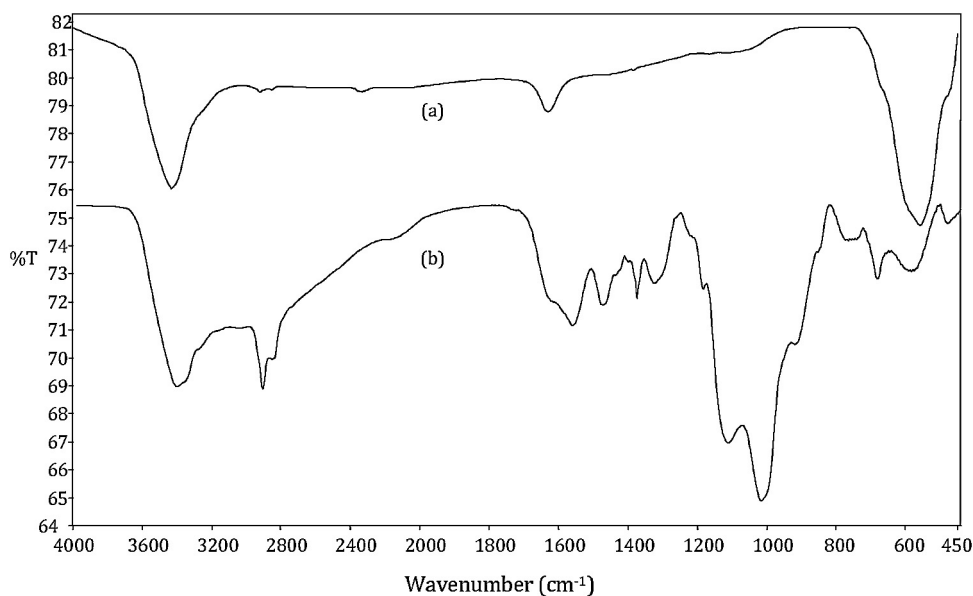


Fig. 6. FT-IR spectrum (a) Manganese ferrite nanoparticle and (b) CSMAN.

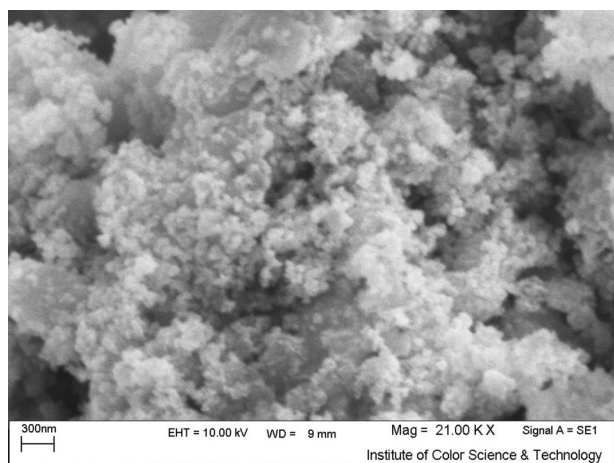


Fig. 7. SEM image of CSMAN.

SEM is an important tool to characterize the surface morphology and physical properties of the adsorbent surface. It is useful to determine the particle shape and appropriate size distribution of the adsorbent. Scanning electron micrograph of magnetic nanoparticle was shown in Fig. 7. The SEM picture of sample showed CSMAN has homogenous particle ( $\leq 100$  nm).

#### 4 Conclusion

In this paper, CSMAN was synthesized and used to remove dye from single and binary systems. Acid Red 18 (AR18), Direct Green 6 (DG6) and Direct Red 31 (DR31) were used as model compounds. Adsorption kinetic of dyes was found to conform to pseudo-second order kinetics. It was found that dye adsorption onto magnetic nanoparticle followed with Langmuir isotherm. At a fixed magnetic nanoparticle dosage, the amount of dye adsorbed increased with increasing dye concentration. Dye removal capacity of magnetic nanoparticle does not decrease in the presence of inorganic anions (salts). The value of  $\alpha$  is close to 1.0. Thus CSMAN has no selectivity. The results showed that the magnetic nanoparticle as a magnetic adsorbent might be used to remove dyes from colored wastewater.

#### References

- [1] N.M. Mahmoodi, *Water Air Soil Pollut.* 224 (2013), art. no. 1612.
- [2] N.M. Mahmoodi, *J. Mol. Catal. A: Chem.* 366 (2013) 254.
- [3] N.M. Mahmoodi, *Mater. Res. Bull.* 48 (2013) 4255.
- [4] C.H.C. Noraini, N. Morad, I. Norli, T.T. Teng, C.J. Ougubue, *Water Air Soil Pollut.* 223 (2012) 5131.
- [5] Z. Aksu, *Process Biochem.* 40 (2005) 997.
- [6] N.M. Mahmoodi, *J. Chem. Eng. Data* 56 (2011) 2802.
- [7] D. Gümüř, F. Akbal, *Water Air Soil Pollut.* 216 (2011) 117.
- [8] N. Atar, A. Olgun, F. Çolak, *Eng. Life Sci.* 8 (2008) 499.
- [9] Y. Bulut, H. Aydin, *Desalination* 194 (2006) 259.
- [10] H. Parab, M. Sudersanan, N. Shenoy, T. Pathare, B. Vaze, *Clean* 37 (2009) 963.
- [11] B. Pan, B. Pan, W. Zhang, L. Lv, Q. Zhang, S. Zheng, *Chem. Eng. J.* 151 (2009) 19.
- [12] B.C. Pan, Q.X. Zhang, F.W. Meng, X.T. Li, X. Zhang, J.Z. Zheng, W.M. Zhang, B.J. Pan, J.L. Chen, *Environ. Sci. Technol.* 39 (2005) 3308.
- [13] K. Zheng, B.C. Pan, Q.J. Zhang, W.M. Zhang, B.J. Pan, Y.H. Han, Q.R. Zhang, W. Du, Z.W. Xu, Q.X. Zhang, *Sep. Purif. Technol.* 57 (2007) 250.
- [14] V. Rocher, J.M. Siaugue, V. Cabuil, A. Bee, *Water Res.* 42 (2008) 1290.
- [15] J.L. Gong, B. Wang, G.M. Zeng, C.P. Yang, C.G. Niu, Q.Y. Niu, W.J. Zhou, Y. Liang, J. Hazard. Mater. 164 (2009) 1517.
- [16] S. Qadri, A. Ganoe, Y. Haik, J. Hazard. Mater. 169 (2009) 318.
- [17] S. Qu, F. Huang, S. Yu, G. Chen, J. Kong, J. Hazard. Mater. 160 (2008) 643.
- [18] K.K.H. Choy, J.F. Porter, G. McKay, *J. Chem. Eng. Data* 45 (2000) 575.
- [19] S. Lagergren, *K. Sven. Vetenskapsakad. Handl.* 24 (1898) 1.
- [20] Y.S. Ho, *Adsorption of Heavy Metals From Waste Streams by Peat*, The University of Birmingham, Birmingham, UK, 1995 (PhD Thesis).
- [21] A. Ozcan, A.S. Ozcan, *J. Hazard. Mater.* 125 (2005) 252.
- [22] S. Senthilkumaar, P. Kalaamani, K. Porkodi, P.R. Varadarajan, C.V. Subburaam, *Bioresour. Technol.* 97 (2006) 1618.
- [23] W.J. Weber, J.C. Morris, *J. Sanit. Eng. Div. Am. Soc. Civil Eng.* 89 (1963) 31.
- [24] N.M. Mahmoodi, *J. Taiwan Inst. Chem. Eng.* 44 (2013) 321.
- [25] M. Uğurlu, *Microporous Mesoporous Mater.* 119 (2009) 276.
- [26] E. Demirbas, M. Kobya, S. Oncel, S. Sencan, *Bioresour. Technol.* 84 (2002) 291.
- [27] N.K. Amin, *Desalination* 223 (2008) 152.
- [28] I. Langmuir, *J. Am. Chem. Soc.* 38 (1916) 2221.
- [29] I. Langmuir, *J. Am. Chem. Soc.* 39 (1917) 1848.
- [30] I. Langmuir, *J. Am. Chem. Soc.* 40 (1918) 1361.
- [31] H.M.F. Freundlich, *Z. Phys. Chem.* 57 (1906) 385.
- [32] M.J. Tempkin, V. Pyzhev, *Acta Physicochim. USSR* 12 (1940) 217.
- [33] Y.C. Kim, I. Kim, S.C. Rengraj, J. Yi, *Environ. Sci. Technol.* 38 (2004) 924.
- [34] G.Z. Kyzas, D.N. Bikiaris, N.K. Lazaridis, *Chem. Eng. J.* 149 (2009) 263.
- [35] G. Crini, C. Robert, F. Gimbert, B. Martel, O. Adam, F. De Giorgi, *J. Hazard. Mater.* 153 (2008) 96.
- [36] G. Crini, P.M. Badot, *Prog. Polym. Sci.* 33 (2008) 399.
- [37] P.K. Dutta, K.D. Bhavani, N. Sharma, *Asian Textile J.* 10 (2001) 57.
- [38] M.S. Chiou, H.Y. Li, *Chemosphere* 50 (2003) 1095.
- [39] S. Chatterjee, S. Chatterjee, B.P. Chatterjee, A.R. Das, A.K. Guha, *J. Colloid Interface Sci.* 288 (2005) 30.
- [40] N.M. Mahmoodi, *Water Air Soil Pollut.* 224 (2013), art. no. 1419.
- [41] D.L. Pavia, G.M. Lampman, G.S. Kaiz, *Introduction to Spectroscopy: A Guide for Students of Organic Chemistry*, W.B. Saunders Company, 1987.
- [42] Z.Y. Yuan, S.Q. Liu, T.H. Chen, J.Z. Wang, H.X. Li, *J. Chem. Soc. Chem. Commun.* 9 (1995) 973.